crystals

MDPI

Article

Development of Composite Scintillators Based on the LuAG: Pr Single Crystalline Films and LuAG:Sc Single Crystals

Vitalii Gorbenko [1,*], Sandra Witkiewicz-Łukaszek [1], Tetiana Zorenko [1], Yuri Syrotych [1], Jiri A. Mares [2], Romana Kucerkova [2], Martin Nikl [2], Oleg Sidletskiy [1,3,4], Alexander Fedorov [5] and Yuriy Zorenko [1,*]

1 Institute of Physics, Kazimierz Wielki University in Bydgoszcz, 85090 Bydgoszcz, Poland; s-witkiewicz@wp.pl (S.W.-Ł.); tzorenko@ukw.edu.pl (T.Z.); yrasyr@gmail.com (Y.S.); osidletskiy@yahoo.com or oleg.sidletskiy@ensemble3.eu (O.S.)
2 Institute of Physics, Academy of Sciences of Czech Republic, Cukovarnicka Str. 10, 16200 Prague, Czech Republic; amares@fzu.cz (J.A.M.); kucerko@fzu.cz (R.K.); nikl@fzu.cz (M.N.)
3 Institute of Scintillation Materials, National Academy of Sciences of Ukraine, 61001 Kharkiv, Ukraine
4 Ensemble3 Sp. z o.o., Wólczynska Str. 133, 01-919 Warszawa, Poland
5 SSI Institute for Single Crystals, National Academy of Sciences of Ukraine, 61178 Kharkiv, Ukraine; fedorov@xray.isc.kharkov.com
* Correspondence: gorbenko@ukw.edu.pl (V.G.); zorenko@ukw.edu.pl (Y.Z.)

Abstract: The scintillation properties of novel type of composite scintillator based on $Lu_3Al_5O_{12}$:Pr (LuAG:Pr) single crystalline film (SCF) and LuAG:Sc substrate grown by the liquid-phase epitaxy method are considered in this work. The registration of α-particles and γ-quanta in such types of composites occurs by means of separation of the scintillation decay kinetics of SCF and crystal parts, respectively. Namely, under excitation by α-particles of ^{241}Am (5.5 MeV) source and γ-quanta of ^{137}Cs (662 keV) source, the large differences in the respective scintillation decay kinetics and decay time values t_α and t_γ are observed for the LuAG:Pr SCF/LuAG:Sc SC composite scintillator with various film thicknesses. Furthermore, the best t_γ/t_α ratio above 4.5 is achieved for such types of epitaxial structure with SCF and substrate thicknesses of 17 μm and about 0.5 mm, respectively. The development types of composite scintillators can be successfully applied for simultaneous registration of α-particles and γ-quanta in the mixed radiation fluxes.

Keywords: composite scintillators; liquid-phase epitaxy; single crystalline films; single crystals; Pr^{3+} and Sc^{3+} dopants

Citation: Gorbenko, V.; Witkiewicz-Łukaszek, S.; Zorenko, T.; Syrotych, Y.; Mares, J.A.; Kucerkova, R.; Nikl, M.; Sidletskiy, O.; Fedorov, A.; Zorenko, Y. Development of Composite Scintillators Based on the LuAG: Pr Single Crystalline Films and LuAG:Sc Single Crystals. *Crystals* **2021**, *11*, 846. https://doi.org/10.3390/cryst11080846

Academic Editor: Ana M. Garcia-Deibe

Received: 20 May 2021
Accepted: 12 July 2021
Published: 22 July 2021

1. Introduction

Nowadays, the liquid-phase epitaxy (LPE) growth technique presents a versatile method for manufacturing the single crystalline film (SCF) scintillators based on various types of oxide materials with different crystallographic structure and cation content [1]. During the last thirty years, the SCF scintillators based on the simple and mixed garnet [1–11], perovskite [1,12], orthosilicate [13–15], pyrosilicates [16] and tungstate [17] compounds, as well as the simple oxides such as sapphire Al_2O_3 [18], lutetia Lu_2O_3 [19] and β-Ga_2O_3 [20], have been developed by using the LPE method.

The LPE method permits us to choose the film scintillator thickness close to the pathway of registering particles in scintillation materials. Namely, the thickness of film scintillators, which are necessary for the complete stopping of α-particles from ^{239}Pu and ^{241}Am sources with an energy of 5.15 and 5.5 MeV, respectively, typically lies in the 12–15 μm range [21]. Furthermore, the LPE technology offers also wide possibility of the development of composite scintillator materials of a "phoswich type" (phosphor sandwich). Such types of scintillators enable separate registration of the various components in the mixed ionization fluxes. Namely, the LPE-grown epitaxial structures of the garnets, containing SCF and substrate scintillators, can be used for registration of α-particles (absorbed only in the SCF part) and γ-rays (stopped mainly in SC substrate). For this reason, the

composite scintillators based on the mentioned epitaxial structures can be used in nuclear research, radiation monitoring, microtomography and many other devices for detection of ionization radiation.

The first example of LPE grown composite scintillators was produced in 1990 [21]. These composite scintillators were based on the epitaxial structures of $Y_3Al_5O_{12}$ (YAG) garnet. Namely, the two types of YAG:Ce SCF/YAG:Nd SC and YAG:Ce SCF/YAG:Sc SC composite scintillators were grown by using the LPE method for simultaneous registration of α- and β-particles, as well as α-particles and X-rays or low-energy γ-quanta [21]. Meanwhile, due to the low density, ϱ = 4.52 g/cm^3, and small effective atomic number, Z_{eff} = 29, the YAG SC substrates can be used only for detection of low-energy types of ionizing radiations.

The LuAG garnet host possesses a significantly higher value, ϱ = 6.7 g/cm^3 and Z_{eff} = 61 in comparison with YAG [22]. For this reason, crystals of LuAG:Ce, LuAG:Pr and LuAG:Sc garnets are the well-known scintillators for radiation monitoring and computer tomography [23,24]. Furthermore, the LuAG host is a very prospective material for the creation of composite scintillators as well. Recently, several types of epitaxial structures based on the Ce^{3+} and Pr^{3+} doped SCFs and Ce^{3+}, Pr^{3+} and Sc^{3+} doped SC of LuAG garnets were successfully grown by using the LPE method, and the scintillation properties of respective composite scintillators were investigated [25–27]. Namely, we confirm in these works that the LuAG:Pr SCF/LuAG:Ce SC, LuAG:Sc SCF/LuAG:Ce SC and (Lu,Tb)AG:Ce SCF/LuAG:Pr SC epitaxial structures can be used for the detection of α-particles and γ-rays by means of the differences in the pulse height spectra and decay kinetics the SCF and SC parts of composite scintillators.

The present work involved searching for the new types of effective composite scintillators for simultaneous registration of the different components of mixed ionizing fluxes, including α-particles and γ-rays with improved functional properties. In this work, we present the results on crystallization and investigation of the optical and scintillation properties of composite scintillators based on the LuAG:Pr SCF/LuAG:Sc SC epitaxial structures grown by the LPE method.

2. Growth of Composite Detectors

The LuAG:Sc substrates with the 10 × 10 mm^2 size and the 0.5 mm thickness were used for creation of the composite scintillators (Figure 1). The substrates were prepared from LuAG:Sc crystals with a Sc concentration of 0.25 at.%, grown by using the Czochralski method in Crutur Ltd., Czech Republic.

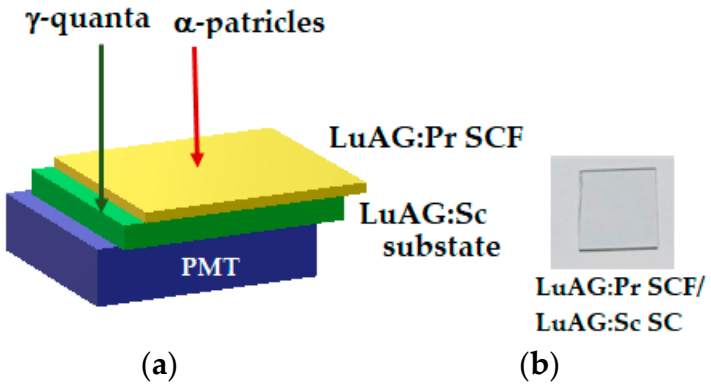

Figure 1. Scheme of LPE grown composite scintillator for registration of α-particles and γ-quanta (**a**) and the sample of LuAG:Pr SCF/LuAG:Sc SC composite scintillator with sizes of 10 × 10 × 0.5 mm^3 prepared by using LPE method (**b**).

The set of LuAG:Pr SCF/LuAG SC composite scintillators was grown by using the LPE method from the super-cooled melt solutions based on the PbO-B_2O_3 flux (see Reference [16] for details). Figure 1 shows an example of the mentioned composite scintillators.

Later, two epitaxial structures with different LuAG:Pr SCF thicknesses (21 and 17 μm), grown onto the LuAG:Sc SC substrates with a thickness of 0.5 mm, were selected for investigation of the scintillation properties of this type of composite scintillators (Table 1).

Table 1. Characteristics of LuAG:Pr SCFs, LuAG:Sc SC substrates and LuAG:Pr SCF/LuAG:Sc SC composite scintillators; h—SCF thickness, T_g—temperature of growth, f—velocity of SCF growth, LY—light yield under α-particles excitation with ^{239}Pu (5.15 MeV) source.

No. of Sample	Type of SCF	Type of Substrate	h, μm	T_g, °C	f, μm/min	LY, %
Crytur		LuAG:Sc	500			95
a0	LuAG:Pr	YAG	19	975	0.19	100
a1	LuAG:Pr	LuAG:Sc	21	1007	0.3	80
a2	LuAG:Pr	LuAG:Sc	17	995	0.66	69

The sample LuAG:Pr SCF was crystalized also onto undoped YAG substrate at relatively the same growth conditions for comparison with the properties of composite scintillators. The growth conditions of the LuAG:Pr SCF and LuAG:Pr SCF/LuAG:Sc SC epitaxial structures, selected for investigation of the content and structural properties, as well for studying their absorption, cathodoluminescent and scintillation properties, were summarized in Table 1.

The structural quality of the composite scintillators was characterized by the X-ray diffraction (Figure 2). From the respective XRD patterns of these SCFs, we can also calculate the lattice constants of the SCF and SC parts of epitaxial structures and estimate the misfit between their lattice constants $m = (a_{SCF} - a_{sub})/a_{sub}*100\%$ (Figure 2a). Namely, the LuAG:Sc substrate and a1 LuAG:Pr SCF possess the lattice constants of 11.9103 Å and 11.9157 Å, respectively, and the SCF/substrate misfit value m = 0.045% (Figure 2a).

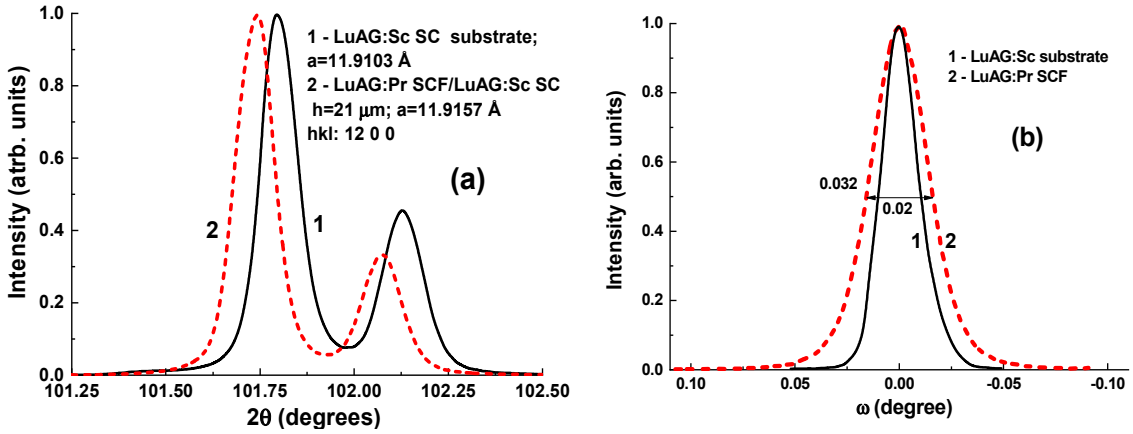

Figure 2. (**a**) XRD patterns of (1200) planes of a1LuAG:Pr SCF grown onto LuAG:Sc substrate with (100) orientation (d); (**b**) rocking curves of a1LuAG:Pr SCF (2) grown onto LuAG:Sc substrate (1).

For study of the uniformity of LuAG:Pr SCFs LPE grown onto LuAG:Sc SC substrates at so small SCF/substrate misfit the rocking curves (RCs) of these samples in the 2θ scan mode were measured and compared (Figure 2b). RCs of the mentioned samples were recorded by using $Cu_{K\alpha}$ radiation in a double crystal spectrometer with a silicon monochromator.

As can be seen from Figure 2b, the RCs of LuAG:Sc and LuAG:Pr substrate show very good symmetry and uniformity of peaks in the ω scan mode. Meanwhile, the FWHM values of RCs for LuAG:Pr SCF are equal to 0.032 degrees, which is 1.6 times larger than FWHM values of 0.02 degrees for the corresponding peaks in LuAG:Sc substrate (Figure 2b). At the same time, the structural quality of the LuAG:Pr SCF, which is proportional to the FWHM of rocking curves, is very high due to lower SCF-substrate misfit values **m.**

3. Experimental Results

The absorption spectra, cathodoluminescence (CL) spectra, scintillation light yield (LY), energy resolution and scintillation decay kinetics measurements under excitation by α–particles and γ-quanta were used for characterization of the properties of LuAG:Sc substrate and two samples LuAG:Pr SCF/LuAG:Sc SC composite scintillators.

The absorption spectra in the 200–1100 nm range were measured using by a UV–Vis Jasco 760 spectrometer. The CL spectra in the 200–925 nm range were measured by using a Stellar Net spectrometer with TE-cooled CCD detector under excitation by electron gun from SEM JEOL JSM-820 electron microscope working at U = 30 kV, I = 0.1 μA. The pulse height spectra (PHS) of all SCFs and SC substrate samples were measured with a shaping time of 12 μs, using the setup based on a Hamamatsu H6521 photomultiplier (PMP) and multi-channel analyzer (MCA) under excitation by α-particles of ^{239}Pu (5.15 MeV) source, and the results of these measurements were used for determination of their scintillation LY (Table 1). Namely, these PHS were compared with the spectra of standard YAG:Ce SCF sample with a photoelectron yield of 360 phels/MeV and a LY of 2650 photons/MeV [17] and also with the reference LuAG:Sc substrate. The scintillation decay kinetics under the mentioned α-particles excitation were measured in the detector based on the Hamamatsu H6521 PMT and digital Tektronix TDS3052 oscilloscope. All the measurements were performed at room temperature (RT).

The scintillation LY and decay kinetics of the selected samples of composite scintillators (see Table 1) were also tested by using the setup based on a HPMT DEP PP0475B hybrid PMT, Ortec 672 spectroscopy preamplifier and 927 ASPEC MCA and PC control. The PHSs were measured under excitation by α-particles of ^{241}Am (5.5 MeV) and γ-rays of ^{137}Cs (662 keV) sources, respectively.

It is worth noting here that the α-particles of ^{239}Pu and ^{241}Am sources absorb only in SCF scintillators because the pathway of α-particles in the studied materials lies in the 12–15 μm range.

3.1. Absorption Spectra

Figure 3 presents the absorption spectra of the LuAG:Pr SCF/LuAG:Sc SC composite scintillators measured in the comparison with the absorption spectra of the LuAG:Pr SCF, grown onto undoped YAG substrate. The E_2 and E_1 absorption bands, peaked at 239 and 284 nm, are related to the allowed 4f-5d^{1,2} transitions of Pr^{3+} ions in LuAG:Pr SCFs. The other absorption bands, which peaked in 260–262 nm and below 200 nm, correspond to the $^1S_0 \rightarrow {}^3P_1$ and $^1S_0 \rightarrow {}^1P_1$ transitions of Pb^{2+} flux impurity in these SCFs, respectively. The absorption spectra of LuAG:Sc substrate show only the wide low-intensive band peaked around 257 nm (Figure 3). Most probably, this absorption band is connected with very common $O^{2-} \rightarrow Fe^{3+}$ charge transfer transitions of Fe^{3+} trace impurity [28,29] in the raw oxides used for LuAG:Pr SC growth.

3.2. Cathodoluminescence Spectra (CL)

The CL spectra of two LuAG:Pr SCF/LuAG:Sc SC composite scintillators with different SCF thicknesses in comparison with CL spectrum of LuAG:Sc substrate are shown in Figure 4. The peaks at 275 nm in CL spectrum LuAG:Sc SC substrate are related to the luminescence of excitons localized and bound with Sc^{3+} isoelectronic impurities in Al^{3+} octahedral positions of the garnet host [21,25]. The CL spectra of LuAG:Sc SC substrate also possess the low-intensive emission band peaked at 595 nm. Most probably, this band corresponds to the luminescence of dimer or more complex charged oxygen vacancies with one or two trapped electrons [30,31]. The luminescence of such centers has been recently observed in several oxide hosts, namely in (Y,Lu)AlO_3 perovskites [31]. Taking into account this assumption, the luminescence of such defect centers in LuAG:Sc SC can be excited via the UV luminescence of Sc^{3+} centers. It is also worth noting that, due to the overlap with the corresponding Pr^{3+} absorption bands (Figure 3), UV light from the LuAG: Sc substrate may be partially reabsorbed by Pr3 + ions in SCF scintillators.

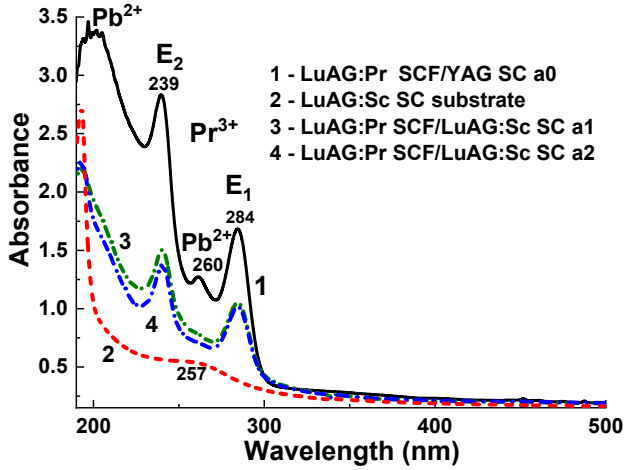

Figure 3. Absorption spectra of LuAG:Pr SCF/LuAG:Sc SC epitaxial structures (3, 4) in comparison with the absorption spectra of LuAG:Pr SCF grown onto YAG substrate (1) and LuAG:Sc substrate (2).

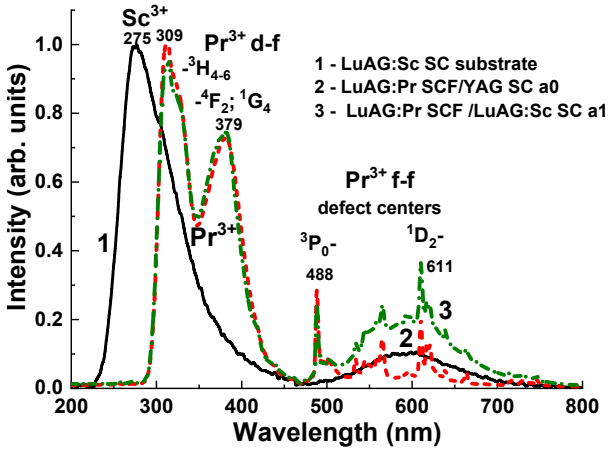

Figure 4. Normalized CL spectra of LuAG:Pr SCF/LuAG:Sc SC composite scintillator (3) in comparison with CL spectra of LuAG:Sc substrate (1) and LuAG:Pr SCF grown onto YAG substrate (2).

The CL spectra of LuAG:Pr SCF and LuAG:Pr SCF/LuAG:Sc SC epitaxial structures (Figure 4, curves 2 and 3) shows two intensive UV emission bands, peaked at 309 and 379 nm, related to the $5d^1$- $4f(^3H_{4\text{-}6}, {}^3H_5, {}^4F_2; {}^1G_4)$ transitions of Pr^{3+} ions. The narrow emission bands in the visible range of LuAG:Pr SCF are related to the 4f-4f transitions of Pr^{3+} ions from $^3P_0$-and $^1D_2$ levels to ^3H_j states. In LuAG:Pr SCF/LuAG:Sc SC epitaxial structures, these sharp Pr^{3+} emission bands overlaps with the wide band of defect centers in LuAG:Sc substrate peaked at 595 nm. Most probably, the luminescence of these defect centers in LuAG:Sc SC is excited by the UV emission of Pr^{3+} ions in the respective LuAG:Pr SCFs.

3.3. Pulse Height Spectra

The PHS of two LuAG:Pr SCF/LuAG:Sc SC composite scintillator samples under excitation by α-particles and γ-ray of ^{241}Am and ^{137}Cs sources are shown in Figure 5a,b, respectively. The main peaks in Figure 5a correspond to the total absorption of α-particles with an energy of 5.5 MeV. The peaks in the left part of the spectrum are related to the absorption of the 59.6 keV low-energy line of ^{241}Am source. The positions and shape of the main photopeaks are slightly different for various SCF and substrate scintillators. This means that α-particles excite only LuAG:Pr SCF parts of composite scintillators. These results on the LY measurements of composite scintillators under α-particle excitation by ^{241}Am source (Figure 5a) are coherent with the LY of these samples under excitation by

^{239}Pu source (Table 1). Meanwhile, the variations in the content of Pb^{2+} flux related impurity in LuAG:Pr SCFs grown from PbO based flux at different temperatures (Table 1) result also in the notable deviation of their scintillation LY (Figure 5a) (see also References [32,33]).

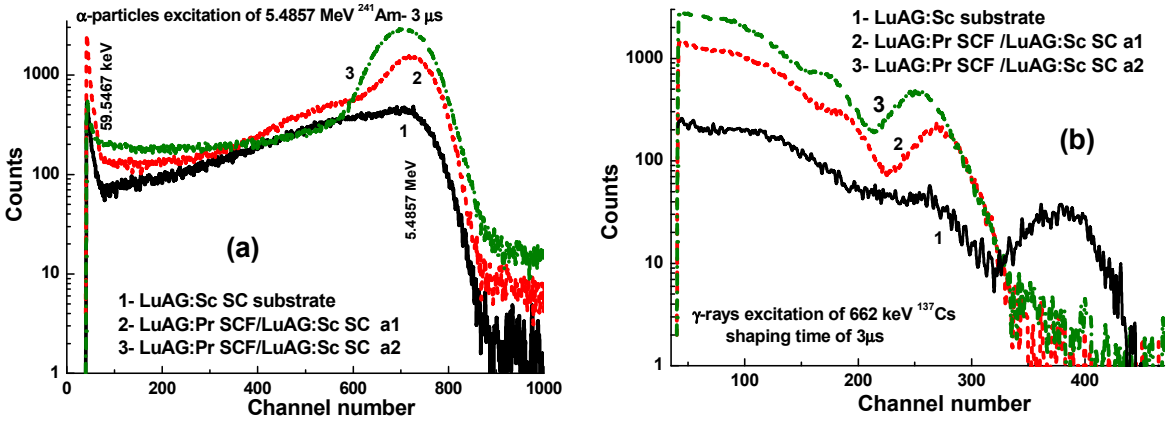

Figure 5. PHS of LuAG:Sc substrate (1) and a1 (2) and a2 (3) samples of LuAG:Pr SCF/LuAG:Sc SC epitaxial structures measured in the 3 μs time interval under α-particle excitation by ^{241}Am (5.5 MeV) source (**a**) and γ-quantum excitation by ^{137}Cs (662 keV) source (**b**).

Under excitation of LuAG:Pr SCF/LuAG:Ce SC composite scintillators by γ-rays from ^{137}Cs source, the significant Compton scattering tools are present in PHS (Figure 5b; see also Reference [27]). Meanwhile, the last peaks in PHS corresponds to the total absorption of γ quanta with an energy of 662 keV (Figure 5b). The low-energy line of ^{137}Cs source corresponds to additional peak at energy of 32 keV.

It is important to note here the different positions of main PHS photopeaks for LuAG:Pr SCF/LuAG:Sc SC epitaxial structures and LuAG:Sc substrate (Figure 5b). This means that γ-rays, apart from excitation of the substrate, excite SCF scintillators as well. For this reason, the total scintillation LY of LuAG:Pr SCF/LuAG:Sc SC composite scintillators under γ-ray excitation will be also affected by LY of SCF scintillators. As a consequence, the position of the main PHS photopeaks corresponding to the absorption of 662 keV quanta of ^{137}Cs source depends notably on the thickness and LY of the SCF scintillators.

It should be noted here that, in the case of excitation of with an energy of 662 keV of the ^{137}Cs radioisotope, the total attenuation coefficient of the LuAG host is ~0.095 cm^2/g [27]. Taking into account the same attenuation factors for the film and the substrate, the LuAG:Pr SCFs with a total thickness of 34–42 μm on both parts of the substrate can absorb gamma quanta in the amount of 6.8–8.5%, compared to 100% for the LuAG substrate with a thickness of 500 μm. Therefore, the effect of influence of SCFs on total scintillation LY and decay kinetics of the tested composite scintillators is predicted a priori.

3.4. LY

The variations of LY (in ph/MeV) of LuAG:Pr/LuAG:Sc epitaxial structures and LuAG:Sc substrate measured within the 0.5–10 μs shaping time interval under α-particle excitation by ^{241}Am (5.5 MeV) and γ-ray excitation by ^{137}Cs (662 keV) are shown in Figure 6a,b, respectively. Furthermore, the values of LY_α and LY_γ and their LY_α/LY_γ ratios for the mentioned scintillators, detected with "fast" (0.5 μs) and "slow" (10 μs) shaping times under α-particles and γ-rays excitation, respectively, are presented in Table 2.

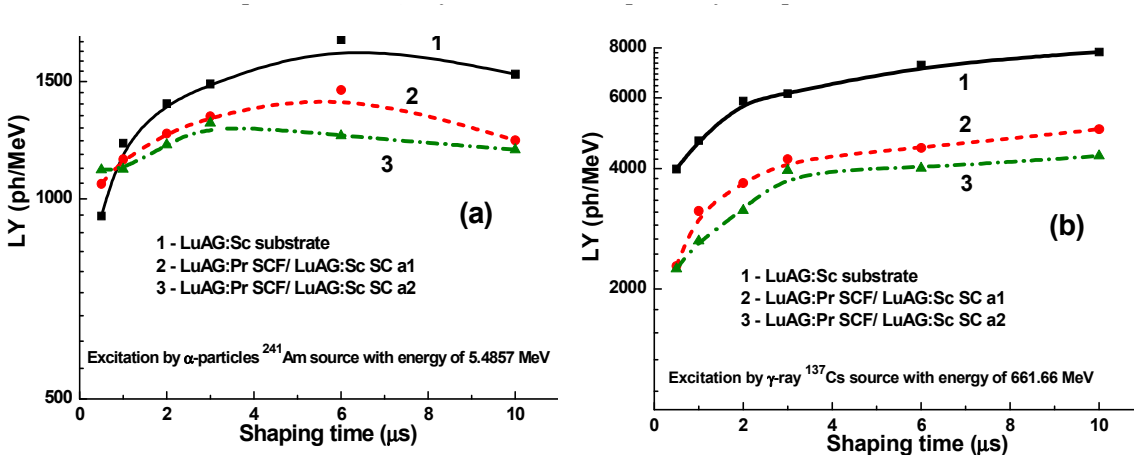

Figure 6. Dependence of LY values for LuAG:Sc SC substrate (1) and of a1 (2) and a2 (3) samples of LuAG:Pr SCF/LuAG:Sc SC epitaxial structure measured under α-particle excitation by ^{241}Am (5.5 MeV) source (**a**) and γ-ray excitation by ^{137}Cs (662 keV) source (**b**).

Table 2. The deviation of LY_α and LY_γ values and LY_α/LY_γ ratios of LuAG:Sc SC substrate and two samples of LuAG:Pr SCF/LuAG:Sc SC composite scintillators measured with shaping times of 0.5 and 10 μs under α-particle and γ-ray excitations.

LY, ph/MeV	Shaping Time, μs	LuAG:Sc SC sub, μs	LuAG:Pr SCF/LuAG:Sc SC a1, μs	LuAG:Pr SCF/LuAG:Sc SC a2, μs
LY_α	0.5	942	1054	1071
LY_α	10	1539	1225	1185
LY_γ	0.5	3988	2284	2246
LY_γ	10	7819	5012	4302
LY_α/LY_γ	0.5	0.23	0.46	0.49
LY_α/LY_γ	10	0.19	0.24	0.52

In the case of α-particles excitation, the maximal LY values of 1735 and 1457 ph/MeV for LuAG:Sc substrate and LuAG:Pr SCF/LuAG:Sc SC a1 epitaxial structure, respectively, are reached at a shaping time of 6 μs (Figure 6a). Meanwhile, in the case of γ-ray excitation, the LY maxima of these scintillators, being equal to 7819 and 5012 ph/MeV, respectively, are reached already at a shaping time of 10 μs (Figure 6b). We have also found that the LY_α/LY_γ value for LuAG:Sc SC scintillator varies in the 0.19–0.23 range within the 0.5–10 μs shaping time interval (Table 2), and such a value is coherent with the value of 0.2 for YAG:Ce SC scintillator [21,27].

3.5. Energy Resolution

The variation of the energy resolution of LuAG:Sc SC substrate and LuAG:Pr SCF/LuAG:Sc SC epitaxial structures, detected with the 0.5–10 μs shaping time under excitation by α-particles and γ-rays, is shown in Figure 7a,b, respectively. As can be seen from Figure 7a, the energy resolution of substrate and a1 composite sample under registration of α-particles shows opposite trend on the LY/shaping time dependences (Figure 6) and lies in the 13.2–30.4% and 14.4–32.3% ranges, respectively. On the contrary, the energy resolution of a2 composite sample at the detection of α-particles shows significantly less variation on the shaping time and lies between 16.1% and 18.4% in whole 0.5–10 ms range. However, under detection of γ-rays, the energy resolution of a1 and a2 composite samples is notably changed within the shaping time and lies in the 13.5–18.7% and 13.8–17.8% ranges, respectively.

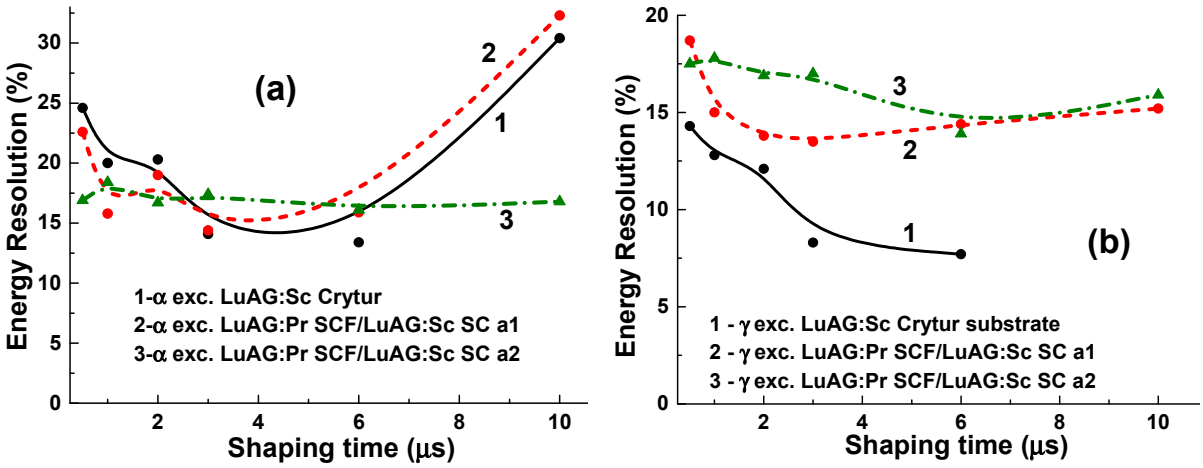

Figure 7. Energy resolution versus shaping time for LuAG:Sc SC substrate (1) and two a1 (2) and a2 (3) samples of LuAG:Pr SCF/LuAG:Sc SC composite scintillators detected within shaping time in the 0.5–10 μs range under excitation by α-particles of ^{241}Am (5.5 MeV) source (**a**) and γ-rays of ^{137}Cs (662 KeV) source (**b**).

Meanwhile, the energy resolution of the LuAG:Sc Sc substrate under detection of γ-rays is notably better and lies in the 7.7–14.3% range (Figure 7b).

3.6. Scintillation Decay Kinetics

In the case of creation of composite scintillators, based on the LPE grown epitaxial structures of garnet compounds, it is very important to analyze firstly the scintillation decay profiles of SC substrates under α-particle and γ-ray excitation in a wide range of decay time and emission intensity. Namely, the scintillation decay kinetics of LuAG:Sc SC substrate under α-particle and γ -ray excitation is presented in Figure 8. The t_α/t_γ or t_γ/t_α ratios of scintillation intensity decay to 1/e, 0.1 and 0.05 levels were used also for description of the difference between the respective scintillation decay profiles under α-particles and γ-quanta excitation (Table 3).

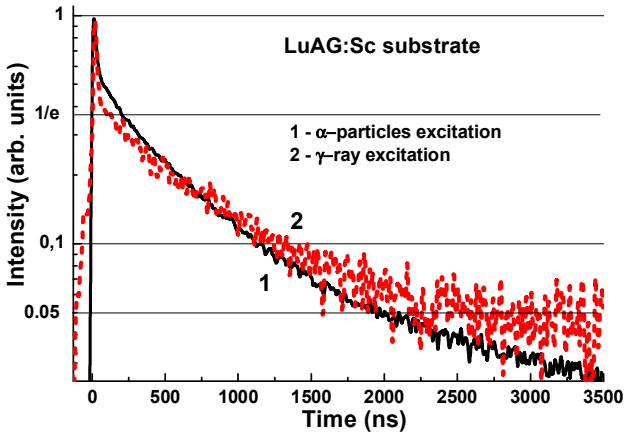

Figure 8. Scintillation decay profiles of LuAG:Sc substrate under α-particle excitation by ^{241}Am (5.5 eV) (1) and γ-quanta by ^{137}Cs (662 KeV) (2) sources.

The rate of separation of the scintillation decay profiles under detection of α-particles and γ-quanta can be significantly improved in the composite scintillators based on the SCFs and crystals of different garnet compounds in comparison with respective crystal-substrates (Figure 9). The following experiments of LuAG:Pr SCF/LuAG:Sc SC LPE grown epitaxial structures confirm such a suggestion. Namely, the separation of the scintillating decay profiles of SCF and SC substrate parts of such composite scintillator can be obtained

in the wide 100–3500 ns time interval, where the scintillation response is significantly faster under γ ray excitation than that under α-particle excitation (Figure 9).

Table 3. Time dependence of intensity of scintillation decay of LuAG:Sc SC substrate from the initial value at t = 0 to 1/e, 0.1 and 0.05 levels.

Intensity	LuAG:Sc Substrate		
	t_α, ns	t_γ, ns	t_α/t_γ or t_γ/t_α Ratio
1/e	208	121	1.72
0.1	1125	1360	1.21
0.05	1982	2646	1.34

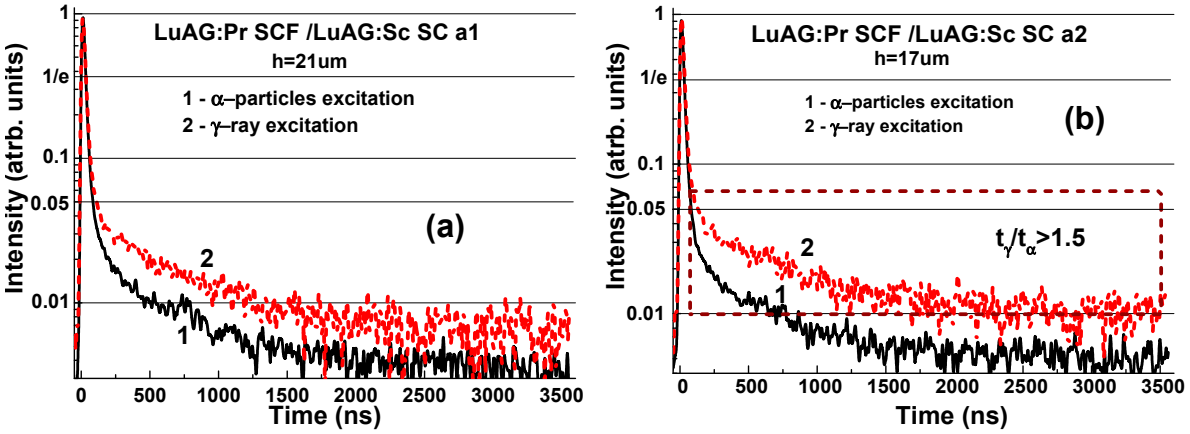

Figure 9. Scintillation decay profiles of a1 (**a**) and a2 (**b**) samples of LuAG:Pr SCF/LuAG:Sc SC composite scintillators with a SCF thickness of 21 and 17 μm, respectively, under α-particle excitation by ^{241}Am (5.5 MeV) source (curves 1) and γ-ray by ^{137}Cs (662 KeV) source (curves 2).

The abovementioned conclusion is illustrated also by comparison of the differences in the decay times of the intensity decay to 1/e, 0.1, 0.05 and 0.01 levels under α-particle and γ-rays excitation (so called ***t_γ/t_α ratio***) in the LuAG:Pr SCF/LuAG:Sc SC composite scintillators and the reference LuAG:Sc substrate (Figure 10 and Table 4). Specifically, for LuAG:Pr SCF/LuAG:Sc SC a2 sample, the t_γ/t_α ratio is significantly large between 1/e to 0.01 levels of intensity decay in comparison with a1 sample (Figure 9). Furthermore, the best separation of the scintillation decay from the SCF and SC parts of such composite scintillator, being equal to t_γ/t_α = 1.55–3.3, can be obtained in the relatively narrow range from 0.065 to 0.01 levels in the time intervals 75–3500 ns, which are shown by the dashed line in Figure 9b.

Table 4. Time dependence of scintillation intensity decay from the initial value at t = 0 to 1/e, 0.1 and 0.05 level for LuAG:Pr SCF/LuAG:Sc SC a1 and a2 composite scintillator samples under α-particle excitation by ^{241}Am source and γ-ray excitation by ^{137}Cs source.

Intensity	a1			a2		
	t_α, ns	t_γ, ns	t_γ/t_α Ratio	t_α, ns	t_γ, ns	t_γ/t_α Ratio
1/e	34.8	36.5	1.04	32.7	37	1.13
0.1	60	65.5	1.09	58	67.4	1.16
0.05	85	107.6	1.26	86	133	1.55
0.01	545	1641	3.01	830	2733	3.3

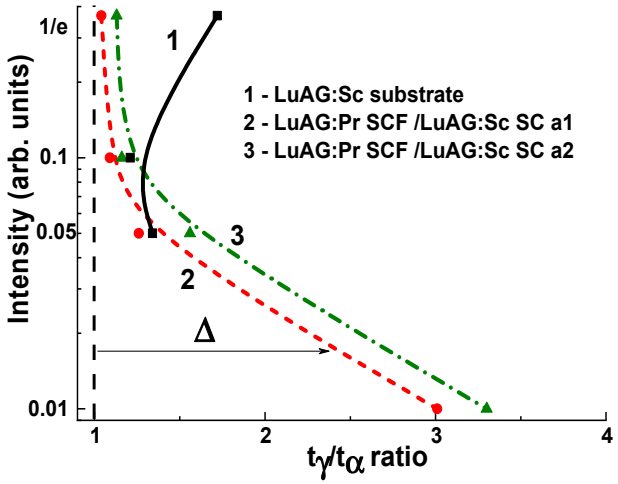

Figure 10. Plots of t_γ/t_α ratio of scintillation decay times under α- and γ-ray excitation vs. the intensity of scintillation decay to 1/e, 0.1, 0.05 and 0.01 levels for LuAG:Sc substrate (curve 1), as well as for a1 (curve 2) and a2 (curve 3) samples of LuAG:Ce SCF/LuAG:Sc SC composite scintillators.

4. Discussion

For analysis of the differences between the decay profiles of composite scintillator under α-particle and γ-ray excitation, the most important value is t_α/t_γ or t_γ/t_α ratio, which needs to be "as large as it is possible" in the broad time interval for the selected combination of scintillation materials used for SCF and substrate parts [21]. It is acceptable that the scintillation response from SCF and substrate scintillators can be readily separated if t_α/t_γ or t_γ/t_α ratio exceeds 1.5 [34]. In this case, the so-called Δ parameter (introduced as difference $t_\gamma/t_\alpha - 1$ for more clear interpretation of the rate of γ/α discrimination) overcomes the 0.5 value (Figure 10). Such a demand is fully filled for the a1 and a2 samples of LuAG:Ce SCF/LuAG:Sc SC epitaxial structures (Figure 10, curves 2 and 3, respectively).

The reasons for the mentioned differences in the separation of the scintillation profiles under α-particle and γ-ray excitations can be related to (i) the different interaction processes of the particles and quanta with the same garnet host and/or to (ii) the different thicknesses of SCF and substrate parts of the composite scintillator. Generally, the shape of scintillation decay profile of epitaxial structure under γ-ray excitation will depend also on the ratio between SCF and substrate thickness and their scintillation LY.

Therefore, the selection of the suitable ratio of thickness of SCF and substrate parts is very important for the optimization of the figure of merit of composite scintillator.

In overall case, it is optimal that the thickness of SCF scintillator is slightly exceeds the penetration depth of detected particles. For SCF of LuAG garnet, such thickness is equal to 12–15 μm for detection of particles with an energy of 5.15–5.5 MeV [11]. In this case, the unwanted absorption of γ-rays by SCF scintillator will be minimal (Figure 11). On the other hand, due to the demand for the absorption of γ-quanta with the energy in the tens-hundreds KeV range, the thickness of LuAG:Sc substrate needs to be "as thick as it is possible". Meanwhile, taking into account the need of stable mounting of thick and heavy substrate in Pt holder for LPE growth, the most optimal thicknesses of LuAG:Sc substrates lie in the 0.5–1 mm range. Taking into account the abovementioned, the optimal values of t_γ/t_α ratio at registration of α-particles and γ-quanta, using LuAG:Pr SCF/LuAG:Sc SC composite scintillator, being equal to 1.55–3.3 at intensity decay from 0.065 to 0.01 levels in the 75–3500 ns time interval, are obtained for the a2 sample with a SCF thickness of 17 μm and a substrate thickness of 0.5 mm (Figure 9b).

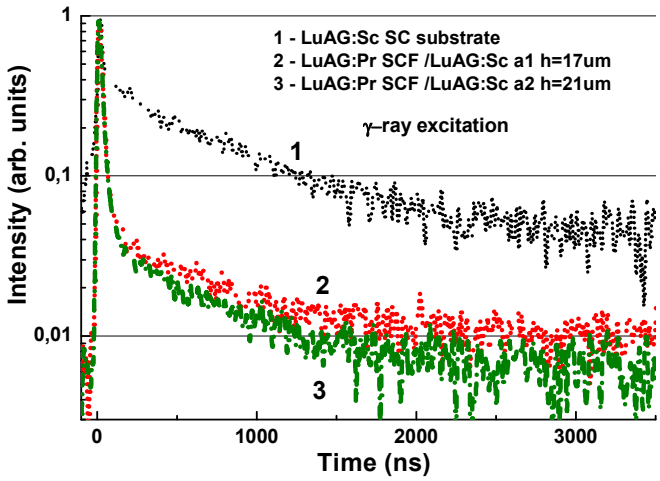

Figure 11. Scintillation decay kinetics of LuAG:Sc substrate (curve 1) and a1 and a2 samples of LuAG:Pr SCF/LuAG:Sc SC composite scintillators with a SCF thickness of 17 and 21 μm (curves 2 and 3, respectively) under γ-ray excitation by ^{137}Cs source with an energy of 661.66 keV.

5. Conclusions

The new type of composite scintillator, based on LuAG:Pr SCFs with the thickness in the 17–21 μm range, and LuAG:Sc substrate with a thickness of 0.5 mm, prepared from the respective single crystal (SC) with a Sc content of 0.25 at.%, was grown by using the LPE method from melt solutions, using PbO-B_2O_3 flux.

The notable differences in the scintillation decay kinetics of LuAG:Pr SCF/LuAG:Sc SC epitaxial structures are observed within the two decades of intensity decay from 1.0 to 0.01 levels in the wide time interval up to 3500 ns under excitation by α–particles by ^{241}Am (5.5 MeV) and γ-quanta by ^{137}Cs (0.662 MeV) sources. Such differences can be characterized by the decay time ratio t_γ/t_α, which, for this type of composite scintillator (at SCF and a substrate thickness of 17 μm and 0.5 mm, respectively), reaches the largest values within t_γ/t_α = 1.55–3.3 range at the intensity decay from the 0.065 level down to 0.01 level in the time interval from 75 to 3500 ns. Such value of t_γ/t_α ratio allows one to easily perform the time discrimination of the signals detected by the SCF and SC parts of composite scintillators. For this reason, the LPE grown LuAG:Pr SCF/and LuAG:Sc SC epitaxial structures can be successfully used for the simultaneous detection of α-particles and γ-rays in the mixed fluxes of ionization radiation.

Author Contributions: V.G. performed SCF growth experiments and wrote growth part of paper; S.W.-Ł. and Y.S. collected and analyzed the SCF optical and scintillation properties; T.Z. measured the scintillation LY and decay kinetics measurements; J.A.M. and R.K. performed pulse height spectra, energy resolution and scintillation decay kinetics measurements; M.N. provide the substrates and analyzed whole experimental materials; O.S. analyzed the scintillation properties of film and composite scintillators; A.F. performed the XRD investigations and analysis of SCF structural quality; Y.Z. analyzed whole experimental materials and wrote Introduction, Fourth part and Conclusion of the paper. All authors have read and agreed to the published version of the manuscript.

Funding: Polish National Science Centre (NCN); Polish National Agency for Academic Exchange (PNAAE), European Structural and Investment Funds; Czech Ministry of Education, Youth and Sports; Czech Science Foundation (GACR).

Acknowledgments: The work was performed in the framework of Polish NCN 2018/31/B/ST8/03390 project (V.G., S.W.Ł.,T.Z., Y.S.) and Polish PNAAE PPN/ULM/2020/1/00298 project (O.S.) as well as partially supported from the Operational Programme Research, Development and Education financed by European Structural and Investment Funds and the Czech Ministry of Education, Youth and Sports (Project No. SOLID21 CZ.02.1.01/0.0/0.0/16_019/0000760) and Czech Science Foundation project 21-17731S (J.A.M., R.K., M.N.). OS acknowledges the scholarship of the Polish National Agency for Academic Exchange under the agreement No. PPN/ULM/2020/1/00298/U/00001.

Conflicts of Interest: The authors declare no conflict of interest.

References

1. Ferrand, B.; Chambaz, B.; Couchaud, M. Liquid phase epitaxy: A versatile technique for the development of miniature optical components in single crystal dielectric media. *Opt. Mater.* **1999**, *11*, 101–114. [CrossRef]
2. Robertson, J.M.; Tol, V.M.V. Cathodoluminescent garnet layers. *Thin Solid Film* **1984**, *114*, 221–240. [CrossRef]
3. Molva, E. Microchip lasers and their applications in optical microsystems. *Opt. Mater.* **1999**, *11*, 289–299. [CrossRef]
4. Koch, A.; Peyrin, F.; Heurtier, P.; Chambaz, B.; Ferrand, B.; Ludwig, W.; Couchaud, M. X-ray camera for computed microtomography of biological samples with micrometer resolution using $Lu_3Al_5O_{12}$ and $Y_3Al_5O_{12}$ scintillators. *Proc. SPIE* **1999**, *3659*, 170.
5. Martin, T.; Koch, A. Recent developments in X-ray imaging with micrometer spatial resolution. *J. Synchrotron Radiat.* **2006**, *13*, 180–194. [CrossRef] [PubMed]
6. Zorenko, Y.; Gorbenko, V.; Zorenko, T.; Vasylkiv, Y. Luminescent properties of the Sc^{3+} doped single crystalline films of (Y, Lu, La)$_3$(Al, Ga)$_5O_{12}$ multi-component garnets. *Opt. Mater.* **2014**, *36*, 1760–1764. [CrossRef]
7. Prusa, P.; Kucera, M.; Mares, J.A.; Onderisinova, Z.; Hanus, M.; Babin, V.; Beitlerova, A.; Nikl, M. Composition tailoring in Ce-doped multicomponent garnet epitaxial film scintillators. *Cryst. Growth Des.* **2015**, *15*, 3715–3723. [CrossRef]
8. Zorenko, Y.; Gorbenko, V.; Zorenko, T.; Popielarski, P.; Mosińska, L.; Fedorov, A. Luminescent and scintillation properties of the Ce^{3+} doped $Y_{3-x}Lu_xAl_5O_{12}$:Ce single crystalline films. *J. Lumin.* **2016**, *169*, 822–827. [CrossRef]
9. Gorbenko, V.; Zorenko, T.; Paprocki, K.; Mahlovanyi, B.; Mazalon, B.; Fedorov, A.; Zhydachevskyy, Y.; Suchocki, A.; Zorenko, Y. Epitaxial growth of single crystalline film scintillators based on the Pr^{3+} doped solid solution of $Lu_3Al_{5-x}Ga_xO_{12}$ garnet. *CrystEngComm* **2017**, *19*, 7031–7040. [CrossRef]
10. Rathaiah, M.; Kučera, M.; Průša, P.; Beitlerová, A.; Nikl, M. Effect of Si^{4+} co-doping on luminescence and scintillation properties of $Lu_3Al_5O_{12}$: Ce, Ca epitaxial garnet films. *Opt. Mater.* **2019**, *91*, 321–325. [CrossRef]
11. Průša, P.; Kučera, M.; Vedda, A.; Fasoli, M.; Moretti, F.; Hanuš, M.; Lučeničová, Z.; Vrba, T.; Nikl, M. Substantial reduction of trapping probability by Mg co-doping in LuAG: Ce, Mg epitaxial garnet films. *J. Lumin.* **2021**, *238*, 118230. [CrossRef]
12. Buryi, M.; Laguta, V.V.; Nikl, M.; Zorenko, T.; Gorbenko, V.; Zorenko, Y. LPE growth and study of the Ce^{3+} incorporation in $LuAlO_3$: Ce single crystalline film scintillators. *CrystEngComm* **2019**, *21*, 3313–3321. [CrossRef]
13. Martin, T.; Douissard, P.-A.; Couchaud, M.; Cecilia, A.; Baumbach, T.; Dupré, K.; Rack, A. LSO-based single crystal film scintillator for synchrotron-based hard X-ray micro-imaging. *IEEE Trans. Nucl. Sci.* **2009**, *56*, 1412–1418. [CrossRef]
14. Rack, A.; Zabler, S.; Mueller, B.R.; Riesemeier, H.; Weidemann, G.; Lange, A.; Goebbels, J.; Hentschel, M.; Goerner, W. High resolution synchrotron-based radiography and tomography using hard X-rays at the BAMline (BESSY II). *Nucl. Instrum. Methods Phys. Res. A* **2008**, *586*, 327–344. [CrossRef]
15. Zorenko, Y.; Gorbenko, V.; Savchyn, V.; Zorenko, T.; Grinyov, B.; Sidletskiy, O.; Fedorov, A.; Mares, J.A.; Nikl, M.; Kucera, M. Lu_2SiO_5:Ce and Y_2SiO_5:Ce single crystals and single crystalline film scintillators: Comparison of the luminescent and scintillation properties. *Radiat. Meas.* **2013**, *56*, 85–89. [CrossRef]
16. Kurosawa, S.; Yoshikawa, A.; Gorbenko, V.; Zorenko, T.; Witkiewicz-Lukaszek, S.; Zorenko, Y. Composite Scintillators Based on the Films and Crystals of $(Lu,Gd,La)_2Si_2O_7$ Pyrosilicates. *IEEE TNS* **2020**, *67*, 994–998. [CrossRef]
17. Zorenko, Y.; Gorbenko, V.; Voznyak, T.; Konstankevych, I.; Savchyn, V.; Batentschuk, M.; Winnacker, A.; Brabec, C.J. Scintillating screens based on the single crystalline films of multicomponent garnets: New achievements and possibilities. *IEEE Trans. Nucl. Sci.* **2012**, *59*, 2281–2285. [CrossRef]
18. Zorenko, Y.; Zorenko, T.; Gorbenko, V.; Savchyn, V.; Voznyak, T.; Fabisiak, K.; Fedorov, A. Zhusupkalieva. Luminescent properties of Al_2O_3:Ce single crystalline films under synchrotron radiation excitation. *Opt. Mater.* **2016**, *59*, 141–144. [CrossRef]
19. Zorenko, T.; Gorbenko, V.; Dulina, N.; Matveevskaya, N.; Yavetskiy, R.; Babayevskaya, N.; Zorenko, Y. Comparative study of the luminescent properties of oxide compounds under synchrotron radiation excitation: Lu_2O_3:Eu nanopowders, ceramics and films. *J. Lumin.* **2018**, *199*, 461–464. [CrossRef]
20. Gorbenko, V.; Galązka, Z.; Zorenko, T.; Paprocki, K.; Witkiewicz, S.; Zorenko, Y. Growth and LPE luminescent and scintillation properties of Ga2O3 based monocrystalline films. *CrystEngComm* **2021**, in press.
21. Zorenko, Y.; Novosad, S.S.; Pashkovskii, M.V.; Lyskovich, A.B.; Savitskii, V.G.; Batenchuk, M.M.; Malyutenkov, P.S.; Patsagan, N.I.; Nazar, I.V.; Gorbenko, V.I. Epitaxial structures of garnets as scintillating detectors of ionizing radiations. *J. Appl. Spectrosc.* **1990**, *52*, 645. [CrossRef]
22. Zorenko, Y.; Gorbenko, V.; Konstankevych, I.; Grinev, B.; Globus, M. Scintillation properties of $Lu_3Al_5O_{12}$:Ce single-crystalline films. *Nucl. Instrum. Methods Phys. Res. A* **2002**, *486*, 309–314. [CrossRef]
23. Nikl, M. (Ed.) *Nanocomposite, Ceramic, and Thin Film Scintillators*; Jenny Stanford Publishing: Singapore, 2017; ISBN 978-981-4745-22-2.
24. Nikl, M.; Yoshikawa, A.; Kamada, K.; Nejezchleb, K.; Stanek, C.R.; Mares, J.A.; Blazek, K. Development of LuAG-based scintillator crystals—A review. *Prog. Cryst. Growth Charact. Mater.* **2013**, *59*, 47–72. [CrossRef]
25. Witkiewicz-Lukaszek, S.; Gorbenko, V.; Zorenko, T.; Paprocki, K.; Sidletskiy, O.; Gerasymov, I.; Mares, J.A.; Kucerkova, R.; Nikl, M.; Zorenko, Y. Composite thermoluminescent detectors based on the Ce^{3+} doped LuAG/YAG and YAG/LuAG epitaxial structures. *IEEE TNS* **2018**, *65*, 2114–2119. [CrossRef]

26. Witkiewicz-Lukaszek, S.; Gorbenko, V.; Zorenko, T.; Paprocki, K.; Sidletski, O.; Gerasymov, I.; Mares, J.A.; Kucerkova, R.; Nikl, M.; Zorenko, Y. Composite scintillators based on the crystals and single crystalline films of LuAG garnet doped with Ce^{3+}, Pr^{3+} and Sc^{3+} ions. *Opt. Mater.* **2018**, *84*, 593–599. [CrossRef]
27. Mares, J.A.; Witkiewicz-Lukaszek, S.; Gorbenko, V.; Zorenko, T.; Kucerkova, R.; Beitlerova, A.; D′Ambrosio, C.; Dlouhy, J.; Nikl, M.; Zorenko, Y. Alpha and gamma spectroscopy of composite scintillators based on the LuAG:Pr crystals and single crystalline films of LuAG:Ce and (Lu,Gd,Tb)AG:Ce garnets. *Opt. Mater.* **2019**, *96*, 109268. [CrossRef]
28. Zorenko, Y.; Batentschuk, M.; Gorbenko, V.; Pashkovsky, M.; Konstankevych, I. Factors determining the energy yield of luminophors based on single-crystal films of Al_2O_3-Y_2O_3-R_2O_3 oxides. *J. Appl. Spectrosc.* **1999**, *66*, 953–959. [CrossRef]
29. Zorenko, T.; Zorenko, Y.; Pavlyk, B.; Turchak, R.; Gorbenko, V.; Konstankevych, I.; Savchyn, V.; Voznyak, T. Influence of thermal treatment and γ-radiation on absorption, luminescence and scintillation properties of $Lu_3Al_5O_{12}$:Ce single crystalline films. *Radiat. Meas.* **2007**, *42*, 557–560. [CrossRef]
30. Zorenko, T.; Gorbenko, V.; Petrosyan, A.; Gieszczyk, W.; Bilski, P.; Zorenko, Y. Intrinsic and defect-related luminescence of $YAlO_3$ and $LuAlO_3$ single crystals and films. *Opt. Mater.* **2018**, *86*, 376–381. [CrossRef]
31. Zorenko, Y.; Zorenko, T.; Voznyak, T.; Mandowski, A.; Qi, X.; Batentschuk, M.; Fridrich, J. Luminescence of F+ and F centers in AI_2O_3-Y_2O_3 oxide compounds. *IOP Conf. Ser. Mater. Sci. Eng.* **2010**, *15*, 012060. [CrossRef]
32. Zorenko, Y.; Batenchuk, M.; Gorbenko, V.; Pashkovsky, M. Single-crystalline oxide films of the Al_2O_3-Y_2O_3-R_2O_3 system as optical sensors of various types of ionizing radiation: Significant advantages over volume analogs. *Proc. SPIE* **1997**, *2967*, 101.
33. Zorenko, Y.; Gorbenko, V.; Voznyak, T.; Savchyn, V.; Nizhankovskiy, S.; Dan'ko, A.; Puzikov, V.; Laguta, V.; Mares, J.A.; Nikl, M.; et al. Luminescent and scintillation properties of $Lu_3Al_5O_{12}$:Sc single crystal and single crystalline films. *Opt. Mater.* **2012**, *34*, 2080. [CrossRef]
34. Gobiein, S. Phoswich Detectors for High Energy Backgrounds. Available online: http://www.detectors.saint-gobain.com (accessed on 29 December 2017).